International Journal of Nanomedicine

Dovepress
open access to scientific and medical research

Open Access Full Text Article

ORIGINAL RESEARCH

Preclinical evaluation of injectable sirolimus formulated with polymeric nanoparticle for cancer therapy

This article was published in the following Dove Press journal:
International Journal of Nanomedicine
26 April 2012
Number of times this article has been viewed

Ha Na Woo[1]*
Hye Kyung Chung[2]*
Eun Jin Ju[1]
Joohee Jung[1,3]
Hye-Won Kang[4]
Sa-Won Lee[4]
Min-Hyo Seo[4]
Jin Seong Lee[5]
Jung Shin Lee[1,6]
Heon Joo Park[7]
Si Yeol Song[1,8]
Seong-Yun Jeong[1]
Eun Kyung Choi[1,2,8]

[1]Institute for Innovative Cancer Research, [2]Center for Development and Commercialization of Anti-cancer Therapeutics, Asan Medical Center, Seoul, [3]College of Pharmacy, Duksung Women's University, Seoul, [4]Department of Parenteral Delivery Program, Samyang Pharmaceuticals R&D, Daejeon, [5]Department of Radiology and Research Institute of Radiology, [6]Department of Internal Medicine, Asan Medical Center, Seoul, [7]Department of Microbiology, College of Medicine, Inha University, Inchon, [8]Department of Radiation Oncology, Asan Medical Center, University of Ulsan College of Medicine, Seoul, Korea

*These authors contributed equally to this study

Correspondence: Eun Kyung Choi
Department of Radiation Oncology, Asan Medical Center, University of Ulsan College of Medicine, Seoul, 138-736, Korea
Tel +82 2 3010 4432
Fax +82 2 486 7258
Email ekchoi@amc.seoul.kr

Seong-Yun Jeong
Institute for innovative Cancer Research, Asan Medical Center, University of Ulsan College of Medicine, Seoul, 138-736, Korea
Tel +82 2 3010 2648
Fax +82 2 3010 2590
Email syj@amc.seoul.kr

Abstract: Nanoparticles are useful delivery vehicles for promising drug candidates that face obstacles for clinical applicability. Sirolimus, an inhibitor of mammalian target of rapamycin has gained attention for targeted anticancer therapy, but its clinical application has been limited by its poor solubility. This study was designed to enhance the feasibility of sirolimus for human cancer treatment. Polymeric nanoparticle (PNP)–sirolimus was developed as an injectable formulation and has been characterized by transmission electron microscopy and dynamic light scattering. Pharmacokinetic analysis revealed that PNP–sirolimus has prolonged circulation in the blood. In addition, PNP–sirolimus preserved the in vitro killing effect of free sirolimus against cancer cells, and intravenous administration displayed its potent in vivo anticancer efficacy in xenograft tumor mice. In addition, PNP–sirolimus enhanced the radiotherapeutic efficacy of sirolimus both in vitro and in vivo. Clinical application of PNP–sirolimus is a promising strategy for human cancer treatment.

Keywords: sirolimus, polymeric nanoparticle, anticancer, radiotherapy

Nanomedicine for diagnostic and therapeutic applications represents an innovative trend in cancer care.[1] Nanoparticles are useful as drug delivery vehicles due to numerous advantages, such as improving drug solubility and stability in serum, extending drug circulation time, enhancing drug bioavailability, and reducing drug toxicity and side effects.[2,3] Nontoxic and biodegradable polymers composed of amphiphilic block copolymers are emerging as powerful drug-delivery vehicles for hydrophobic drugs.

The mammalian target of rapamycin (mTOR) pathway plays a key role in cellular growth, proliferation, and homeostasis.[4] Since mTOR-mediated signaling is frequently upregulated in tumor cells, and inhibition of this pathway induces apoptotic and autophagic cell death of tumor cells, mTOR has been an attractive target for anticancer drug development.[5,6] Sirolimus (Rapamune®; Pfizer, New York City, NY) is a US Food and Drug Administration (FDA)-approved mTOR inhibitor currently used to prevent the rejection of solid organ transplants.[7] Recently, it was reported that sirolimus has antiproliferative and antiangiogenic properties in a variety of tumor cell lines. In addition, other mTOR inhibitors (CCI-779, RAD001, and AP23575) have been evaluated as anticancer therapies against various tumors.[8–11] While early clinical trials suggest promising anticancer activity,[9,12] the clinical development of sirolimus has been hindered by its pharmacokinetical limitations.

Sirolimus is a strongly hydrophobic drug. Consequently, injectable formulations of sirolimus are difficult to prepare and, as a result, sirolimus is only available in oral formulations. However, its oral bioavailability is only about 17%.[13] Therefore, it is

restrictively suitable for low-dosage treatment, such as immunosuppression in renal and liver transplant recipients.[14] These are the potential drawbacks for delivery of sirolimus by conventional dosage formulations.

Since cancer is caused by multiple events, combinational modalities may provide better responses to cancer therapy. Combination treatments of irradiation and chemotherapeutic agents that increase sensitivity to radiation enhance therapeutic efficacy with minimal side effects. In this study, we report a formulation of sirolimus that does not require organic co-solvents or surfactants for solubility using a diblock copolymer. Polymeric nanoparticle-containing sirolimus (PNP–sirolimus) shows improved pharmacokinetic characteristics, potent antitumor activity, and yielded superior results on tumor growth inhibition, especially in combination with radiation.

Materials and methods

Preparation of sirolimus-incorporated polymeric nanoparticles

PNP–sirolimus was prepared by a simple fabrication method using a diblock copolymer, polyethylene glycol–poly-L-lactic acid (mPEG–PLA), monovalent metal salt of a biodegradable polyester (D,L-PLACOONa), and calcium chloride as described previously.[15] Briefly, mPEG–PLA (Mn = 2.0–1.8 KD; 1650 mg), D,L-PLACOONa (Mn = 1.5 KD; 825 mg), and sirolimus (25 mg) were completely dissolved in 1.5 mL of dichloromethane to obtain a clear solution. Dichloromethane was removed on a rotary evaporator under reduced pressure to produce a polymer–drug matrix. Distilled water was added to the matrix and the mixture was stirred for 30 minutes at 50°C, resulting in a mixed polymeric micelle (mPM) solution. To produce the ionically-fixed polymeric nanoparticles, an aliquot of a 100 mg/mL solution of calcium chloride was added to the mPM solution, and the mixture was stirred for 5 minutes at room temperature. D-Mannitol (20%, w/w) aqueous solution was added to the polymeric nanoparticle solution and was stirred for 5 minutes at room temperature. The solution was passed through a 0.22 μm poly(vinylidene fluoride) (PVDF) membrane filter. The filtered solution was freeze-dried and stored in a refrigerator until use. The sirolimus content was determined by high-performance liquid chromatography (HPLC) (Hewlett Packard series 1100; Hewlett Packard, Palo Alto, CA).

Polymeric nanoparticle characterization

Morphological examination of the polymeric nanoparticles was performed by transmission electron microscopy (CM-30; Philips, Eindhoven, The Netherlands). The particle size and zeta potential of the PNPs were measured by laser light scattering (Nano ZS; Malvern Instruments, Malvern, United Kingdom).

Pharmacokinetic study

Male Sprague-Dawley (SD) rats each received a single intravenous dose of 10 mg/kg of sirolimus or PNP–sirolimus and underwent whole blood collections for 48 hours. Serial sirolimus whole blood concentrations (ng/mL) were measured by HPLC with tandem mass spectroscopy (MS/MS). For this, 0.3 mL of whole blood (three samples per group) was collected at 0, 15, and 30 minutes and 1, 2, 4, 8, 24, and 48 hours after administration of sirolimus or PNP–sirolimus. Blood samples were centrifuged within 30 minutes of collection and plasma samples (0.15 mL) were loaded onto a Zorbax XDB-C18 column (2.1 × 100 × 3.5 mm) (Agilent, Santa Clara, CA). Separations were conducted using two solvent systems composed of methanol/ammonium sulfate buffer (99:1, v/v). The flow rate was 0.3 mL/min. Tacrolimus was used as the internal standard for calibration and quality control. All experiments were performed following the protocol approved by the Institutional Animal Care and Use Committee of the Asan Institute for Life Science.

Cell culture

Human lung adenocarcinoma A549 and human breast adenocarcinoma MCF7 cells were maintained in Dulbecco's Modified Eagle's Medium (Gibco-Invitrogen, Carlsbad, CA). Human non-small cell lung cancer NCI-H460 and human metastatic breast cancer MDA-MB-231 cells were maintained in RPMI 1640 medium (Gibco-Invitrogen). Both media were supplemented with 10% fetal bovine serum (Gibco-Invitrogen) and 1% penicillin/streptomycin under a humidified atmosphere of 5% CO_2 and 95% air at 37°C.

Cell proliferation assay

Cells in exponential growth were harvested and plated in 96-well plates (10,000 cells/well in 100 mL of growth medium). Each treatment condition was performed in triplicate. Cells were incubated overnight, and sirolimus or PNP–sirolimus was added to the media. Cells were incubated at 37°C for 48 hours and then processed for the CCK-8 assay (Dojindo Molecular Technologies, Gaithersburg, MD) according to the manufacturer's instructions. After incubation of cells with the CCK-8 reagent for 2 hours, absorbance at 450 nm was measured using a spectrophotometer. To assess the radiosensitization effects, A549 cells were plated in

96-well culture plates 1 day before treatment and treated with PNP–sirolimus (100 nM) only or in combination with radiation (2 or 5 Gy). At 24 and 48 hours after radiation, cell viability was evaluated using the CCK-8 assay. Cells grown in normal culture medium were used as a control for all other samples. Considering the average growth in this control group as 1, relative cell proliferation was calculated.

In vitro clonogenic assay

A clonogenic assay was used to determine the proliferative potential of a cell population by testing the ability of single cells to form colonies in vitro.[16] Colony formation was analyzed by plating 300 cells (sirolimus or PNP–sirolimus) or 50 cells (control or PNP) per well in six-well culture plates. Cells were treated with sirolimus (30 nM), PNP–sirolimus (30 nM), PNP, or saline. For radiosensitizing-effect analysis, cells were irradiated with 0 to 10 Gy. At 2 hours postradiation, cells were treated with 30 nM of sirolimus, PNP–sirolimus, PNP, or saline and then incubated at 37°C for 14 days. Colonies were stained with 0.5% crystal violet (Sigma-Aldrich, St Louis, MO) in methanol. Stained colonies were washed with water, air-dried, and counted when they consisted of more than 50 cells. The surviving fraction was calculated as (mean colonies counted)/[(cells plated) × (plating efficiency)], where plating efficiency was defined as (mean colonies counted)/(cells plated). All values were normalized to untreated cells. The mean number of colonies from triplicates and their standard deviations were calculated.

In vivo tumor growth delay

A549 cells were used as a xenograft model in male athymic nude mice (nu/nu; 6 weeks old; Japan SLC, Hamamatsu, Japan).[17] A suspension of 1×10^6 cells in a 50 mL volume was injected subcutaneously (sc) into the right hindlimb of mice. Tumors were grown for 2 weeks until average tumor volume reached 70~80 mm^3. Mice were then divided into groups (6 mice per group). Treatment groups consisted of control, PNP, and PNP–sirolimus. Mice were treated with 20 mg/kg of PNP–sirolimus by intravenous (iv) injection three times per week for 4 weeks or once per week for 4 weeks. Body weights and tumor volumes were monitored during the course. For analysis of radiosensitization, the radiation groups received 10 Gy of radiation fractionated over 5 consecutive days (from days 1 to 5) using a 6 MV X-ray from linear accelerators (CL/1800; Varian Medical System, Palo Alto, CA) in combination with 5 mg/kg of PNP–sirolimus. Tumor volume was calculated using the formula $V = (L \times W2) \times 0.5$, where V = volume, L = length, and W = width. The results were expressed as the mean ± standard deviation. Statistical analysis was performed using the Mann–Whitney test, and *P* values of 0.005 or less were considered statistically significant. All experiments were performed following the protocol approved by the Institutional Animal Care and Use Committee of the Asan Institute for Life Science.

Western blot analysis

Proteins were separated by gel electrophoresis on a sodium dodecyl sulfate–polyacrylamide gel and then transferred to PVDF membranes. The membranes were blocked with Tris-buffered saline containing 0.1% Tween-20 (TBST) and 5% (w/v) skim milk.[18] After being washed with TBST, the membranes were incubated overnight at 4°C with a phospho-p70S6K or p70S6K antibody (R&D systems, Minneapolis, MN) diluted with TBST containing 1% skim milk. After washing with TBST, the membranes were incubated for 1 hour at room temperature with the secondary antibody (Jackson ImmunoResearch Laboratories, West Grove, PA). Bands were detected by an ECL system. The LC3 antibody was purchased from Novus Biologicals (Littleton, CO).

Results

Preparation of polymeric nanoparticles

Most approaches for the preparation of polymeric nanospheres using amphiphilic block copolymers, such as emulsification or nanoprecipitation, are complex and time-consuming processes that present difficulties for large-scale production.[19,20] In addition, the resulting nanospheres from these techniques have a large particle size and wide size distribution makes sterile filtration difficult. Previously, we reported that mPEG–PLA and D,L-PLACOONa could form mixed polymeric micelles.[21] In addition, a stable metal ion-fixed polymeric nanoparticle (PNP) could be prepared using $CaCl_2$, due to the electrostatic interaction between D,L-PLACOO- and Ca^{2+}, forming a complex of $(D,L\text{-}PLACOO)_2Ca^{2+}$ in aqueous solution. This water-soluble biopolymer is biodegradable and biocompatible.[15] PNP can solubilize 0.2~10 mg/mL concentrations of sirolimus in normal saline. PNP or PNP–sirolimus was highly monodispersed (Figure 1A and B). The smooth surfaces and spherical shape topology of PNPs were confirmed by transmission electron microscopy (TEM). Dynamic light scattering (DLS) analysis revealed that the PNP had a unimodal size distribution with an average hydrodynamic diameter of 34.95 nm having PDI 0.236 and a negative zeta potential of –2.96 mV (Figure 1C; Table 1).

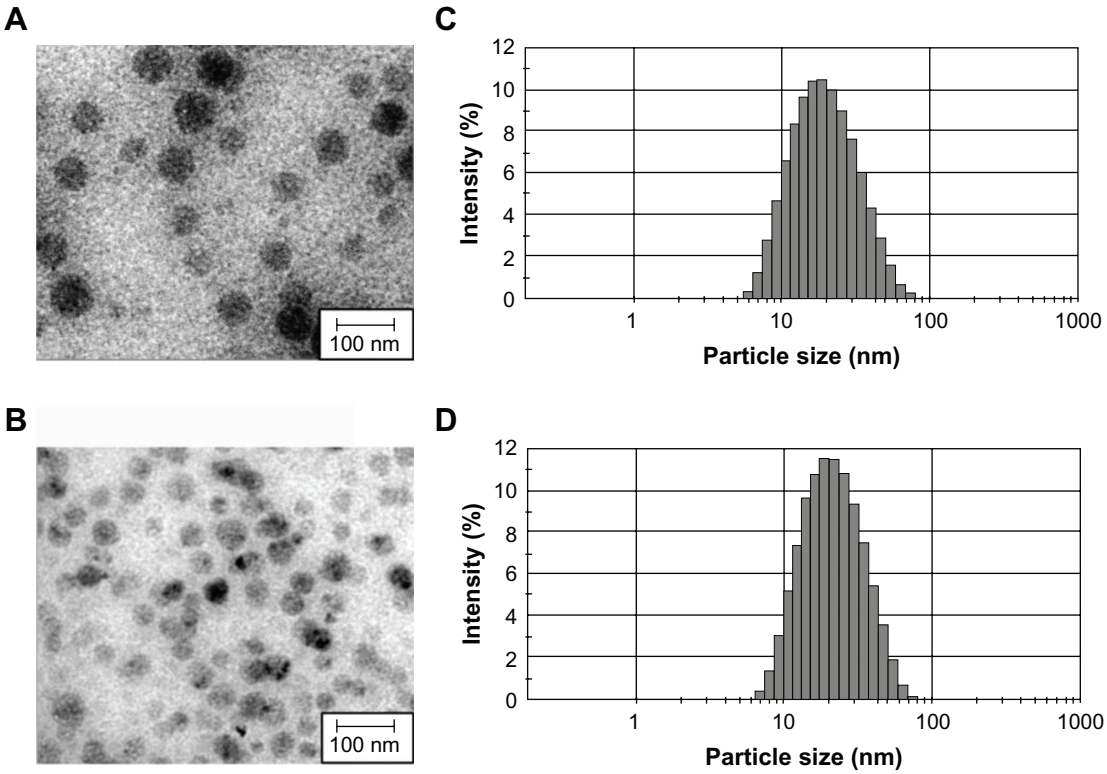

Figure 1 TEM image and hydrodynamic size distribution of (**A** and **C**) PNP and (**B** and **D**) PNP–sirolimus.
Abbreviations: PNP, polymeric nanoparticle; TEM, transmission electron microscopic.

A small increase in size (from 34.95 to 37.83 nm) and zeta potential (from −2.96 to −1.85 mV) was observed following sirolimus encapsulation to PNP (Figure 1D; Table 1).

Pharmacokinetic characterization of PNP–sirolimus

To determine whether PNP–sirolimus shows therapeutic advantages over the free drug, we performed a pharmacokinetic study. Using the same dose (10 mg/kg), noncompartmental pharmacokinetic values of the area under the curve (AUC), the maximum measured drug concentration (C_{max}), the time of peak concentration measured (T_{max}), and the absolute bioavailability (F) were calculated from plasma drug concentration–time data (Figure 2). Detectable plasma concentrations of sirolimus persisted for 48 hours in rats treated with PNP–sirolimus. As shown in Table 2, the T_{max} was the same at 0.25 hours for both free sirolimus and PNP–sirolimus, whereas PNP–sirolimus yielded a significantly higher C_{max} in plasma compared to free sirolimus. A distinct increase in sirolimus concentration was evident at 24 hours on a semi-log concentration time profile after the administration of PNP–sirolimus. Also, PNP–sirolimus provided ~3-fold higher F values in blood compared to free sirolimus. Compared to other administration methods, the C_{max} and AUC were highest on iv PNP–sirolimus (data not shown). Thus, the pharmacokinetic characteristics of PNP–sirolimus were considerably improved compared with free sirolimus.

Table 1 Characterization of PNP nanoparticles for particle size, zeta potential, and PDI

Formulation	Particle size (nm)	PDI	Zeta potential (mV)
PNP vehicle	34.95	0.236	−2.96
PNP–sirolimus	37.83	0.153	−1.85

Abbreviations: PDI, Polydispersity Index; PNP, polymeric nanoparticle.

In vitro anticancer efficacy of PNP–sirolimus

To investigate the cytotoxic effect of PNP–sirolimus against human cancer cells, human lung cancer A549 and NCI-H460 cells and human breast cancer MCF7 and MDA-MB-231 cells were incubated for 48 hours with PNP, PNP–sirolimus, or sirolimus. PNP–sirolimus reduced the proliferation rate of cancer cells by approximately 20% in the case of A549 and MCF7 cells exposed to 500 nM (Figure 3A). The extent of growth inhibition of PNP–sirolimus was similar to that of free sirolimus. For the management of breast cancer, the expression level of estrogen receptor (ER) is an important

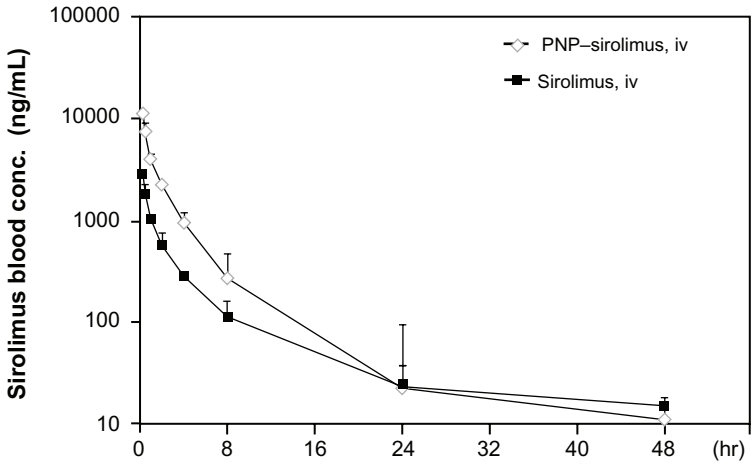

Figure 2 Pharmacokinetic characterization of PNP–sirolimus.
Notes: Plasma concentration-time profiles were determined in Sprague–Dawley rats iv injected with sirolimus (solid square) or PNP–sirolimus (open diamond) at a dose of 10 mg/kg. Experimental points are the means of the observed plasma levels (mean ± SD, n = 3 per group).
Abbreviations: PNP, polymeric nanoparticle; iv, intravenous.

predictive and prognostic factor. PNP–sirolimus displayed similar growth inhibition in ER-positive breast cancer MCF-7 and ER-negative breast cancer MDA-MB231 cells. To evaluate the prolonged effects of PNP–sirolimus on cancer cell survival, a clonogenic assay was performed. A marked decrease in the survival rate of cells treated with PNP–sirolimus or sirolimus was shown in all cancer cell lines (Figure 3B). These results indicate that PNP–sirolimus preserved the cytotoxic effect of sirolimus and exerts potent anticancer effects in human cancer cells.

To explore whether the anticancer effect of PNP–sirolimus occurs through inhibition of the mTOR pathway, we examined the effect of PNP–sirolimus on the phosphorylation of the downstream target p70S6K at Thr389 in A549 cells. As shown in Figure 3C, p70S6K was phosphorylated in normal conditions, which indicates activation of the mTOR-mediated signaling pathway. As expected, the phosphorylation of the downstream effector p70S6K was significantly decreased by PNP–sirolimus, suggesting that PNP–sirolimus effectively inhibits mTOR signaling in a dose-dependent manner.

Table 2 Pharmacokinetic parameters in Sprague–Dawley rats following intravenous injection of sirolimus or PNP–sirolimus

PK parameter	Free sirolimus (iv)	PNP–sirolimus (iv)
AUC_{last} (μg·hours/mL)	5366.7	16,901.7
C_{max} (μg/mL)	2890	11,303.3
T_{max} (hours)	0.25	0.25
F (%)	100	315

Abbreviations: AUC, area under the curve; C_{max}, peak plasma concentration; F, absolute bioavailability; iv, intravenous; PNP, polymeric nanoparticle; T_{max}, time to peak plasma concentration.

In vivo anticancer efficacy of PNP–sirolimus

The in vivo anticancer effect of PNP–sirolimus was evaluated in a xenograft mouse model bearing A549 tumors. To examine the therapeutic activity of PNP–sirolimus as a single agent without toxicity, mice were treated with PNP–sirolimus (20 mg/kg) by iv injection three times per week for 4 weeks or once per week for 4 weeks. Tumor volume and body weight were monitored during the course of the experiment to determine therapeutic efficacy and toxicity. In the control group, the volume of tumors on day 41 was ninefold larger than that of day 1, while the tumor volume of the group treated with PNP–sirolimus was only 1.5-fold higher at three treatments per week, and threefold at one treatment per week (Figure 4A and C). The anticancer effect of PNP–sirolimus was observed starting on day 6 after treatment ($P < 0.005$) and sustained until termination of both experiments. During the experiment, iv drug treatment was well-tolerated, and there was no apparent toxicity throughout the study as evaluated by body weight changes (Figure 4B and D).

In vitro radiosensitization by PNP–sirolimus

Radiation therapy is employed extensively for treatment of almost all types of solid tumors. The use of molecularly-targeted agents in combination with ionizing radiation (IR) is a promising therapeutic strategy against cancer.

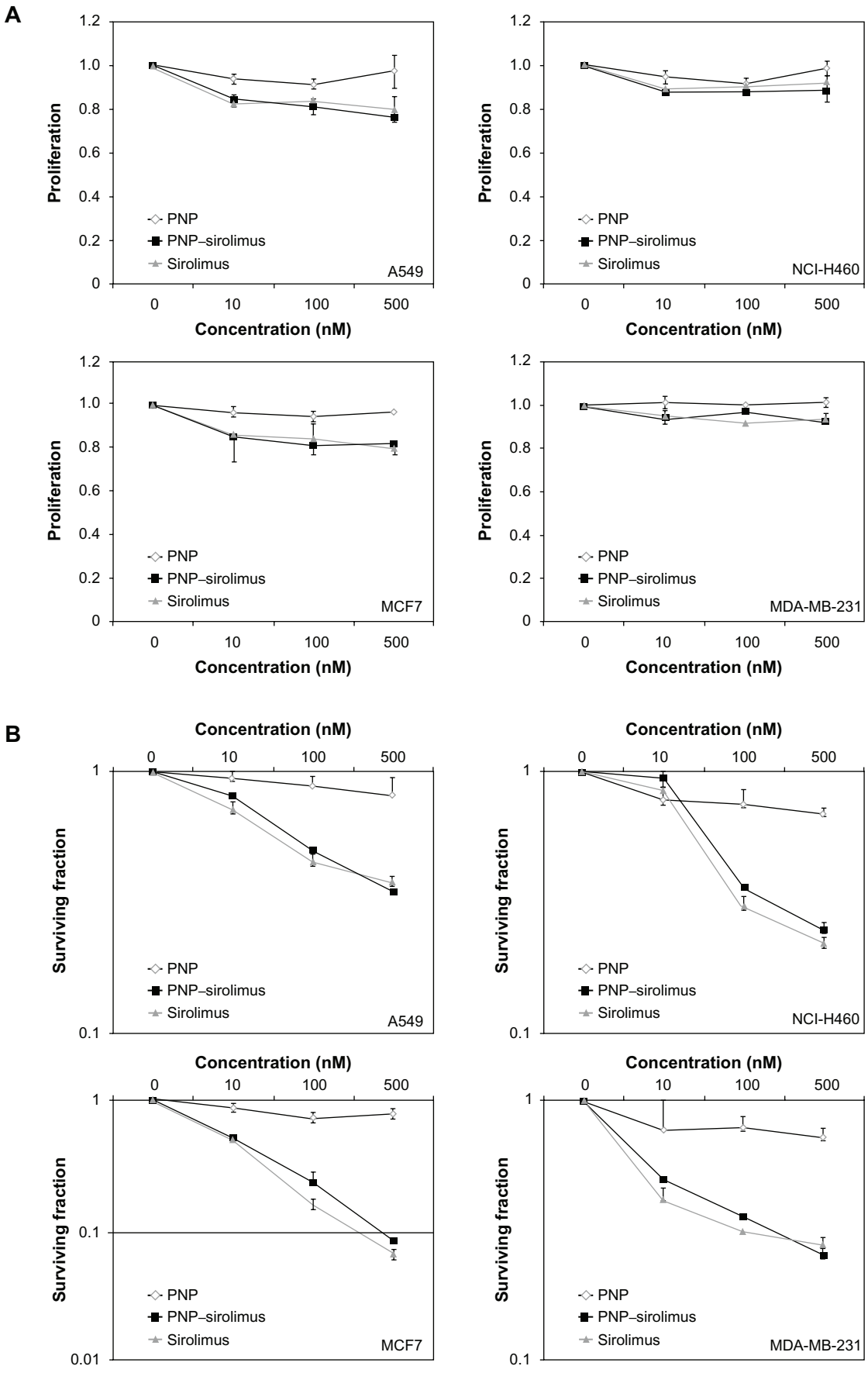

Figure 3 (*Continued*)

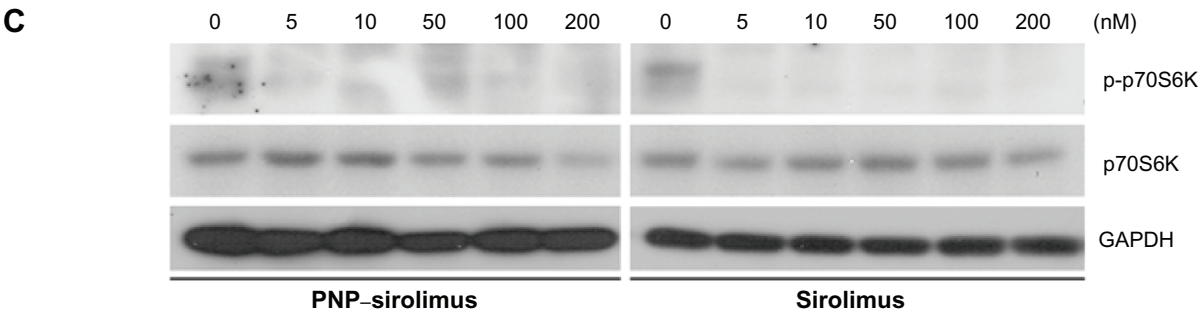

Figure 3 In vitro anticancer efficacy of PNP–sirolimus. (**A**) A549, NCI-H460, MCF7, and MDA-MB-231 cells were incubated with various concentrations of PNP–sirolimus or sirolimus for 48 hours. (**B**) The cellular proliferation rate was measured by a CCK-8 assay. (**C**) The survival fraction was determined by a clonogenic assay. (**D**) Western blot analysis for total and phosphorylated p70S6K protein was performed with GAPDH as a loading control.
Abbreviations: GAPDH, glyceraldehyde-3-phosphate dehydrogenase; PNP, polymeric nanoparticle.

Increasing evidence now indicates that mTOR inhibitors have radiosensitizing effects.[22–24] To determine whether PNP–sirolimus sensitizes A549 cell lines to radiation therapy, CCK-8 and clonogenic assays were performed. Co-treatment of PNP–sirolimus with IR enhanced the radiation-induced cytotoxicity compared with single use of PNP–sirolimus (Figure 5A). A clonogenic assay showed that combined treatment of PNP–sirolimus and IR resulted in enhanced radiosensitivity, although no significant difference was observed between PNP–sirolimus and free sirolimus (Figure 5B).

It is known that mTOR inhibition confers radiosensitivity and induces the nonapoptotic cell death pathway of autophagy.[22] We investigated whether treatment with PNP–sirolimus in combination with IR induces autophagic cell death in A549 cells. Autophagy correlated with increased expression of LC3II, which is an autophagosome formation marker.[25] Western blot analysis was performed to detect the conversion of LC3I into LC3II. A significant increase in LC3II protein is shown in Figure 5C, suggesting that combined therapy of PNP–sirolimus and IR induces autophagic cell death by efficient inhibition of mTOR. We also assessed apoptosis by flow cytometry using annexin V and propidium iodide staining to confirm whether apoptotic cell death was involved. No increased annexin V staining portion was found

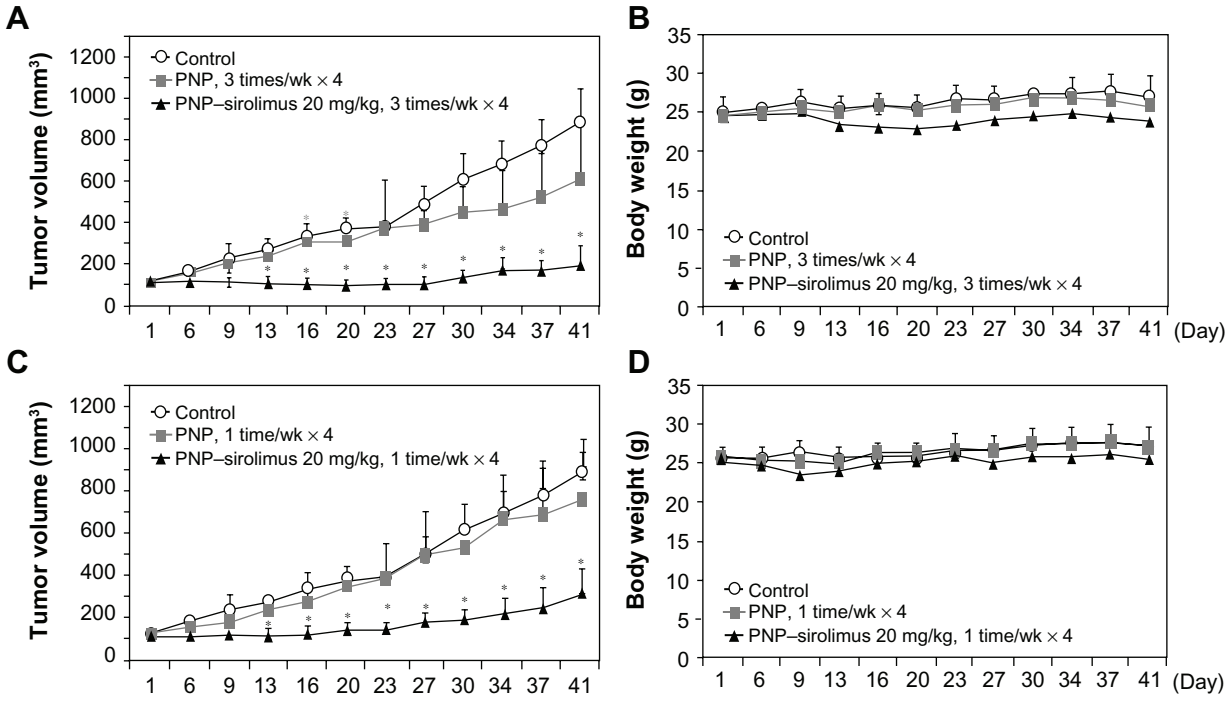

Figure 4 In vivo anticancer efficacy of PNP–sirolimus. (**A**) A549 tumor-bearing mice were treated with 20 mg/kg of PNP–sirolimus three times per week for 4 weeks by iv injection. Tumor volume was measured using a caliper (n = 6; *$P < 0.005$). (**B**) Body weight was monitored twice per week. (**C**) A549 tumor-bearing mice were treated with 20 mg/kg of PNP–sirolimus once per week for 4 weeks by iv injection (n = 6; *$P < 0.005$). (**D**) Body weight was monitored twice per week.
Abbreviations: PNP, polymeric nanoparticle; iv, intravenous.

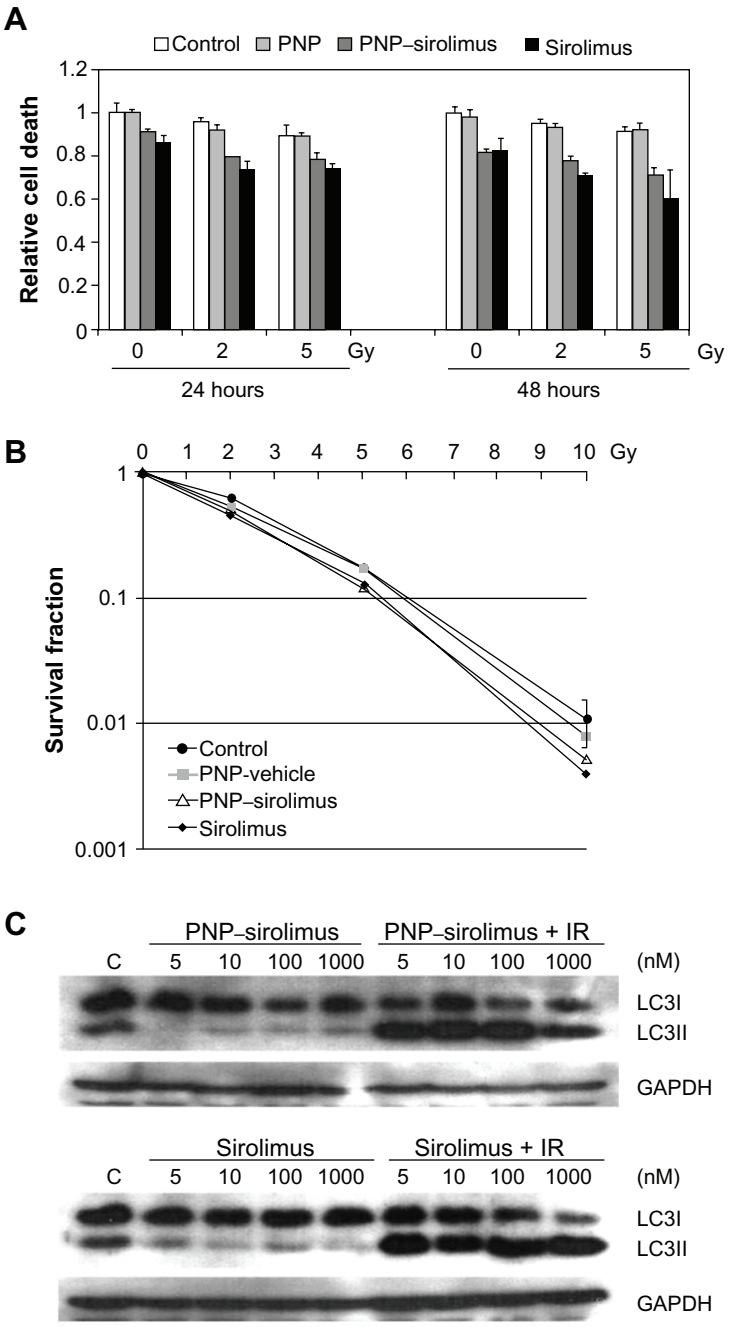

Figure 5 In vitro radiosensitization using PNP–sirolimus. (**A**) A cellular proliferation was measured 24 or 48 hours after PNP–sirolimus and radiation treatment by a CCK-8 assay. (**B**) The survival fraction of PNP–sirolimus in combination with IR was determined by a clonogenic assay. (**C**) Western blot analysis for LC3 proteins was performed. C represents the untreated control. GAPDH was used as the loading control.
Abbreviations: GAPDH, glyceraldehyde-3-phosphate dehydrogenase; IR, ionizing radiation; PNP, polymeric nanoparticle.

in either PNP–sirolimus or free sirolimus, suggesting that cell death caused by these drugs was mainly independent on apoptosis (data not shown).

In vivo radiosensitization by PNP–sirolimus

As for the experiments showing the in vitro radiosensitizing effect of PNP–sirolimus, xenograft mice bearing A549 tumors were employed to validate the in vivo radiosensitizing effect by iv injected PNP–sirolimus. Mice were treated with PNP–sirolimus (5 mg/kg), followed 2 hours later by IR (2 Gy) daily for 5 days. At the dose of 5 mg/kg, PNP–sirolimus alone showed a clear tumor growth delay comparable to that of IR treatment. Combination therapy with PNP–sirolimus and IR was significantly more effective than either IR or PNP–sirolimus alone (Figure 6A) ($n = 6$; $P < 0.005$). There was

no obvious change in the weight of mice after treatments (Figure 6B). Therefore, PNP–sirolimus exerts a potent in vivo anticancer efficacy in xenograft tumor animals, especially when it is combined with radiation.

Discussion

Drug-delivery systems can improve several crucial properties of free drugs, such as solubility, stability, pharmacokinetics, biodistribution, and efficacy.[26] Polymeric micelles or nanoparticles composed of biocompatible and biodegradable materials have been extensively explored as powerful drug-delivery vehicles for cancer drug therapy. In this study, a new polymeric nanoparticle system was prepared by self-assembly of amphiphilic diblock copolymers to solubilize sirolimus in aqueous solutions.

mTOR was discovered in the early 1990s in studies on the mechanism of action of sirolimus, which was originally used as an antifungal agent and later recognized for its anticancer properties.[9,27] Signaling through the mTOR pathway has been linked to growth, progression, and chemoresistance of several cancers and is hyperactivated in certain cancers,[28–30] suggesting mTOR as an attractive target for cancer therapy. Although the inhibition of mTOR by sirolimus is a promising anticancer strategy, its clinical applications have been hindered by its extremely low solubility in water (2.6 mg/mL).[31,34] Sirolimus contains no functional groups that are ionizable in the pH range of 1–10 and is only slightly soluble in acceptable parenteral excipients, such as ethanol, propylene glycol, glycerine, polysorbate 80, and polyethylene glycol 400.[32] Attempts to develop an injectable formulation of sirolimus employing surfactants were not favorably evaluated due to vehicle toxicity. Consequently, previous attempts to develop iv formulations have been difficult, but have allowed for the development of currently employed oral solutions and tablet

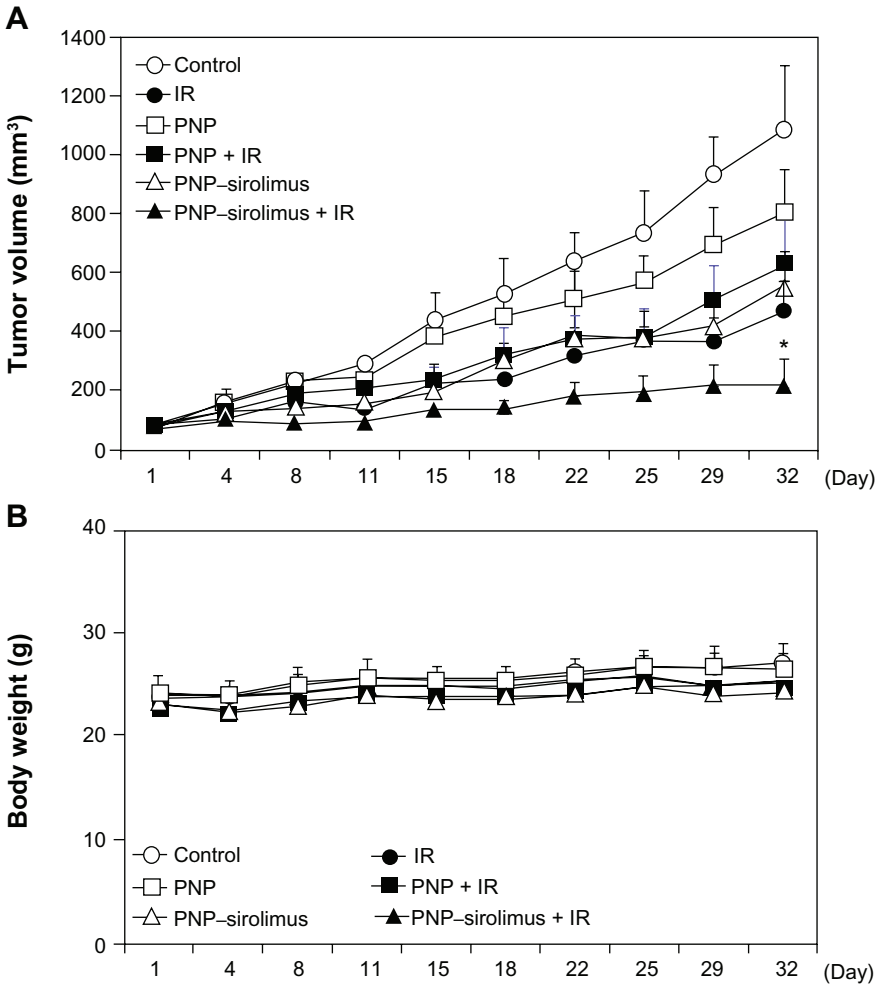

Figure 6 In vivo radiosensitization by PNP–sirolimus. Athymic nude mice with A549 xenograft tumors were treated with PNP or PNP–sirolimus (5 mg/kg), followed 2 hours later by radiation (2 Gy) for 5 consecutive days. (**A**) Average tumor volumes of six mice per group are shown. Error bars represent SD. Statistical analysis was performed using the Mann–Whitney test. *P* values < 0.005 were considered statistically very significant. *$P = 0.0022$. (**B**) Body weight of PNP–sirolimus and/or ionizing radiation-treated mice are shown.

Abbreviations: IR, ionizing radiation; PNP, polymeric nanoparticle; SD, standard deviation.

formulations. To apply sirolimus to human cancer treatment, development of an injectable formulation is required. Recent approaches have been taken to improve the formulation and delivery of sirolimus. One of these approaches was the development of temsirolimus (CCI-779), a water-soluble sirolimus ester that has shown promise in early Phase I trials.[33] However, its iv formulations require ethanol due to the limited solubility of CCI-779, even at 120 mg/mL, which may cause hemolysis.[34]

PNP composed of amphiphilic block copolymers with nontoxic and biodegradable polymers (mPEG–PLA and D,L-PLACOONa) is a powerful drug-delivery vehicle for hydrophobic drugs. PNP exhibited good water solubility for sirolimus (0.2~10 mg/mL). In addition, iv-injected PNP–sirolimus was well tolerated in mice and rats. The PDI of samples demonstrates a unimodal size distribution (Figure 1, Table 1). Positively charged nanoparticles are known to be rapidly cleared from the bloodstream, making them undesirable for drug delivery. In contrast, the zeta potential of PNP–sirolimus was negative. Noncompartmental analysis of the blood concentrations showed a significant change in certain pharmacokinetic parameters of sirolimus in PNP–sirolimus compared to that of control free sirolimus (Figure 2, Table 2). C_{max} and AUC_{last} values were markedly increased, and the absolute bioavailability of PNP–sirolimus was threefold higher. According to our unpublished data, the AUC of PNP–sirolimus increased in a dose-dependent manner. Also, AUC_{last}, C_{max}, and F values were greatest in iv-injected PNP–sirolimus compared to sc or oral administration. Thus, PNP improved the pharmacokinetic characteristics of sirolimus.

In addition, there may be increasing accumulation of PNP–sirolimus at the tumor site because tumor-targeting nanoparticles have enhanced permeability and retention (EPR), which results from the disordered, leaky vasculature of the tumor.[35] To avoid filtration by the kidneys or drug removal by the liver, nanocarriers need to be larger than 10 nm and smaller than 100 nm. PNP–sirolimus has a suitable size (38 nm) for effective delivery and accumulation in tumors. Indeed, the EPR effect will be more effective if nanocarriers circulate for a long period. A common method to protect nanocarriers from the reticuloendothelial system is coating the surface of the particles with PEG. PNP–sirolimus was also coated with PEG molecules by mPEG–PLA during polymer production, which contributes to the increased circulation time of PNP–sirolimus.

Previous studies have shown that sirolimus acts as a cytostatic agent by arresting the cell cycle.[29] PNP–sirolimus had a similar cytotoxicity to the free drug, but showed low cytotoxicity (~20%) in cancer cell lines (Figure 3A). Although tumor cells were not immediately killed by sirolimus, the affected clones did not grow continually. A marked decrease in the survival curve of PNP–sirolimus-treated cells was seen in a clonogenic assay (Figure 3B). We also found that combined treatment of PNP–sirolimus and IR slightly enhanced radiosensitivity in clonogenic assays as compared to either agent alone in vitro (Figure 5B), while it led to a significant in vivo tumor growth delay in the human lung cancer A549 xenograft tumor model (Figure 6). Although we were not able to compare the effect of PNP–sirolimus to that of the free drug in vivo due to the lack of a soluble formulation when free, the pharmaceutical activity of sirolimus when combined with PNP was well preserved as it was evident that the effect of the PNP–sirolimus is very similar to that of the free sirolimus in in vitro results. The remarkable in vivo anticancer and radiosensitization effect could be explained by the EPR effect of PNP–sirolimus. To exclude the possible influence of the PNP vehicle itself on cell viability, various concentrations of PNP vehicle were incubated for 72 hours with A549 cells, and cell viability was assessed. The PNP vehicle had no obvious adverse effect on cell viability (data not shown), demonstrating that the PNP vehicle itself has no cytotoxicity.

Recent cancer treatment usually involves combinations of different modalities in order to maximize the therapeutic outcome and to reduce side effects. Radiation therapy is employed extensively for treatment of almost all types of solid tumors. Despite recent advances in radiotherapy and chemotherapy, the mortality rate of certain cancers, such as lung cancer, remains high. Finding agents that sensitize tumor cells to radiation would increase the tumor response while allowing lower therapeutic doses to be used, thereby minimizing toxicity to surrounding organs. It is well known that mTOR inhibition induces autophagy, which is important in cancer development and progression.[22] PNP–sirolimus and IR lead to enhanced radiosensitization via induction of autophagy in a nonsmall cell lung tumor xenograft model.

In this study, we developed a novel injectable formulation of sirolimus using PNP that consists of biodegradable, biocompatible polymers. This drug could be readily dispersed in physiological media without any surfactants or cosolvents. PNP–sirolimus showed improved pharmacokinetic features compared to free sirolimus. In addition, PNP–sirolimus effectively inhibited tumor cell proliferation and tumor mass growth and enhanced radiation-induced cell death by inhibition of the mTOR pathway and activation of

autophagy. Therefore, clinical application of the injectable PNP–sirolimus may be an attractive new therapeutic approach for cancer therapy.

Acknowledgments

This work was supported by a grant from the Korean Health Technology R&D Project, Ministry for Health and Welfare, Republic of Korea (A062254 and A102059), the Nuclear R&D program through the Korea Science and Engineering Foundation funded by the Ministry of Education, Science and Technology of Korea (2008-03876), the Basic Science Research Program through the National Research Foundation of Korea (NRF) funded by the Ministry of Education, Science and Technology (KRF-2008-313E00444), and a grant from the ASAN Institute for Life Science, Seoul, Korea (2009-445).

Disclosure

The authors report no conflicts of interest in this work.

References

1. Peer D, Karp JM, Hong S, Farokhzad OC, Margalit R, Langer R. Nanocarriers as an emerging platform for cancer therapy. *Nat Nanotechnol*. 2007;2(12):751–760.
2. Ferrari M. Cancer nanotechnology: opportunities and challenges. *Nat Rev Cancer*. 2005;5(3):161–171.
3. Farokhzad OC, Langer R. Impact of nanotechnology on drug delivery. *ACS Nano*. 2009;3(1):16–20.
4. Ciuffreda L, Di Sanza C, Incani UC, Milella M. The mTOR pathway: a new target in cancer therapy. *Curr Cancer Drug Targets*. 2010;10(5):484–495.
5. Sun SY, Rosenberg LM, Wang X, et al. Activation of Akt and eIF4E survival pathways by rapamycin-mediated mammalian target of rapamycin inhibition. *Cancer Res*. 2005;65(16):7052–7058.
6. Liu Q, Thoreen C, Wang J, Sabatini D, Gray NS. mTOR mediated anti-cancer drug discovery. *Drug Discov Today Ther Strateg*. 2009;6(2):47–55.
7. Kahan BD, Camardo JS. Rapamycin: clinical results and future opportunities. *Transplantation*. 2001;72(7):1181–1193.
8. Hoy SM, McKeage K. Temsirolimus: in relapsed and/or refractory mantle cell lymphoma. *Drugs*. 2010;70(14):1819–1829.
9. Panwalkar A, Verstovsek S, Giles FJ. Mammalian target of rapamycin inhibition as therapy for hematologic malignancies. *Cancer*. 2004;100(4):657–666.
10. Wang Y. Everolimus in renal cell carcinoma. *Drugs Today (Barc)*. 2010;46(8):557–566.
11. Adjei AA, Hidalgo M. Intracellular signal transduction pathway proteins as targets for cancer therapy. *J Clin Oncol*. 2005;23(23):5386–5403.
12. Guertin DA, Sabatini DM. The pharmacology of mTOR inhibition. *Sci Signal*. 2009;2(67):pe24.
13. Dias VC, Yatscoff RW. An in vitro method for predicting in vivo oral bioavailability of novel immunosuppressive drugs. *Clin Biochem*. 1996;29(1):43–49.
14. Maramattom BV, Wijdicks EF. Sirolimus may not cause neurotoxicity in kidney and liver transplant recipients. *Neurology*. 2004;63(10):1958–1959.
15. Lee SW, Chang DH, Shim MS, Kim BO, Kim SO, Seo MH. Ionically fixed polymeric nanoparticles as a novel drug carrier. *Pharm Res*. 2007;24(8):1508–1516.
16. Franken NA, Rodermond HM, Stap J, Haveman J, van Bree C. Clonogenic assay of cells in vitro. *Nat Protoc*. 2006;1(5):2315–2319.
17. Jeong SY, Park SJ, Yoon SM, et al. Systemic delivery and preclinical evaluation of Au nanoparticle containing beta-lapachone for radiosensitization. *J Control Release*. 2009;139(3):239–245.
18. Jeong SY, Yi SL, Lim SK, et al. Enhancement of radiotherapeutic effectiveness by temperature-sensitive liposomal 1-methylxanthine. *Int J Pharm*. 2009;372(1–2):132–139.
19. Gref R, Luck M, Quellec P, et al. 'Stealth' corona-core nanoparticles surface modified by polyethylene glycol (PEG): influences of the corona (PEG chain length and surface density) and of the core composition on phagocytic uptake and plasma protein adsorption. *Colloids Surf B Biointerfaces*. 2000;18(3–4):301–313.
20. Avgoustakis K, Beletsi A, Panagi Z, et al. Effect of copolymer composition on the physicochemical characteristics, in vitro stability, and biodistribution of PLGA-mPEG nanoparticles. *Int J Pharm*. 2003;259(1–2):115–127.
21. Kim SC, Kim DW, Shim YH, et al. In vivo evaluation of polymeric micellar paclitaxel formulation: toxicity and efficacy. *J Control Release*. 2001;72(1–3):191–202.
22. Albert JM, Kim KW, Cao C, Lu B. Targeting the Akt/mammalian target of rapamycin pathway for radiosensitization of breast cancer. *Mol Cancer Ther*. 2006;5(5):1183–1189.
23. Cao C, Subhawong T, Albert JM, et al. Inhibition of mammalian target of rapamycin or apoptotic pathway induces autophagy and radiosensitizes PTEN null prostate cancer cells. *Cancer Res*. 2006;66(20):10040–10047.
24. Shinohara ET, Cao C, Niermann K, et al. Enhanced radiation damage of tumor vasculature by mTOR inhibitors. *Oncogene*. 2005;24(35):5414–5422.
25. Aoki H, Kondo Y, Aldape K, et al. Monitoring autophagy in glioblastoma with antibody against isoform B of human microtubule-associated protein 1 light chain 3. *Autophagy*. 2008;4(4):467–475.
26. Allen TM, Cullis PR. Drug delivery systems: entering the mainstream. *Science*. 2004;303(5665):1818–1822.
27. Guba M, von Breitenbuch P, Steinbauer M, et al. Rapamycin inhibits primary and metastatic tumor growth by antiangiogenesis: involvement of vascular endothelial growth factor. *Nat Med*. 2002;8(2):128–135.
28. Wan X, Helman LJ. The biology behind mTOR inhibition in sarcoma. *Oncologist*. 2007;12(8):1007–1018.
29. Guertin DA, Sabatini DM. Defining the role of mTOR in cancer. *Cancer Cell*. 2007;12(1):9–22.
30. Sabatini DM. mTOR and cancer: insights into a complex relationship. *Nat Rev Cancer*. 2006;6(9):729–734.
31. Morris RE. In vivo immunopharmacology of the macrolides FK 506 and rapamycin: toward the era of rational immunosuppressive drug discovery, development, and use. *Transplant Proc*. 1991;23(6):2722–2724.
32. Simamora P, Alvarez JM, Yalkowsky SH. Solubilization of rapamycin. *Int J Pharm*. 2001;213(1–2):25–29.
33. Temsirolimus: CCI 779, CCI-779, cell cycle inhibitor-779. *Drugs R D*. 2004;5(6):363–367.
34. Raymond E, Alexandre J, Faivre S, et al. Safety and pharmacokinetics of escalated doses of weekly intravenous infusion of CCI-779, a novel mTOR inhibitor, in patients with cancer. *J Clin Oncol*. 2004;22(12):2336–2347.
35. Maeda H. Tumor-selective delivery of macromolecular drugs via the EPR effect: background and future prospects. *Bioconjug Chem*. 2010;21(5):797–802.